ACS OMEGA

http://pubs.acs.org/journal/acsodf

Article

Chemical Investigation of *Tetradium ruticarpum* Fruits and Their Antibacterial Activity against *Helicobacter pylori*

Myung Woo Na,[⊥] Se Yun Jeong,[⊥] Yoon-Joo Ko, Dong-Min Kang, Changhyun Pang, Mi-Jeong Ahn, and Ki Hyun Kim*

Cite This: *ACS Omega* 2022, 7, 23736−23743

Read Online

ACCESS | Metrics & More | Article Recommendations | Supporting Information

ABSTRACT: The fruit of *Tetradium ruticarpum*, known as *Evodiae* Fructus, is a traditional herbal medicine used to treat gastric and duodenal ulcers, vomiting, and diarrhea. The traditional usage can be potentially associated with the antibacterial activity of *T. ruticarpum* fruits against *Helicobacter pylori*. However, so far, the antibacterial activity of *T. ruticarpum* fruits and antibacterial components against *H. pylori* has not been investigated despite the traditional folk use. The current study was conducted to investigate the bioactive chemical components of *T. ruticarpum* fruits and evaluate their antibacterial activity against *H. pylori*. Phytochemical investigation of the EtOH extract of *T. ruticarpum* fruits led to the isolation and identification of nine compounds (**1**−**9**), including phellolactone (**1**), the absolute configuration of which has not yet been determined. The chemical structures of the isolated compounds were elucidated by analyzing the spectroscopic data from one-dimensional (1D) and two-dimensional (2D) NMR and high-resolution electrospray ionization mass spectrometry (HR-ESIMS) experiments. Specifically, the absolute configuration of compound **1** was established by the application of computational methods, including electronic circular dichroism (ECD) calculation and the NOE/ROE-based interproton distance measurement technique via peak amplitude normalization for the improved cross-relaxation (PANIC) method. In the anti-*H. pylori* activity test, compound **3** showed the most potent antibacterial activity against *H. pylori* strain 51, with 94.4% inhibition (MIC_{50} and MIC_{90} values of 22 and 50 μM, respectively), comparable to that of metronidazole (97.0% inhibition, and MIC_{50} and MIC_{90} values of 17 and 46 μM, respectively). Moreover, compound **5** exhibited moderate antibacterial activity against *H. pylori* strain 51, with 58.6% inhibition (MIC_{50} value of 99 μM), which was higher than that of quercetin (34.4% inhibition) as a positive control. Based on the bioactivity results, we also analyzed the structure−activity relationship of the anti-*H. pylori* activity. Conclusion: These findings demonstrated that *T. ruticarpum* fruits had antibacterial activity against *H. pylori* and could be used in the treatment of gastric and duodenal ulcers. Meanwhile, the active compound, 1-methyl-2-(8*E*)-8-tridecenyl-4(1*H*)-quinolinone (**3**), identified herein also indicated the potential application in the development of novel antibiotics against *H. pylori*.

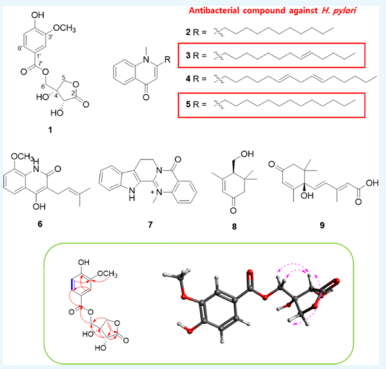

1. INTRODUCTION

Tetradium ruticarpum (A. Juss.) Hartley is a small shrub native to temperate and tropical regions of Asia, including China and Korea, and its dried nearly ripe fruit, also known as *Evodiae* Fructus or *Wu zhu yu* in Chinese, has been used as a traditional herbal medicine for more than 2000 years to treat gastric and duodenal ulcers, headache, abdominal pain, vomiting, diarrhea, dysmenorrhea, and postpartum hemorrhage.[1,2] The fruit of *T. ruticarpum* was first recorded in "Shennong's Classic of Materia Medica", and the fruit of *T. ruticarpum* is named variously in Pharmacopoeias (e.g., Evodia fruit in Korean Pharmacopoeia, Euodia fruit in Japanese Pharmacopoeia, Euodiae fructus in Chinese Pharmacopoeia).[1] However, *T. ruticarpum* has also been reported to exhibit potential toxicity by long-term use or excessive doses, and owing to its toxicity, *T. ruticarpum* is usually processed and/or combined with other herbs in the formulation of traditional Chinese medicine.[2]

Recent pharmacological studies of *T. ruticarpum* fruit have demonstrated that the extracts of *T. ruticarpum* fruit and its active constituents show diverse therapeutic efficacies, including antiproliferative,[3] anti-inflammatory,[4] antibacterial,[5] cytotoxic,[5] antiadipogenic,[6] antioxidant,[7] central nervous system homeostasis,[8] and cardiovascular protective activities.[9] To date, more than 160 chemical components, including alkaloids, terpenoids, steroids, limonoids, phenylpropanoids, flavonoids, phenolic acids, anthraquinones, and essential oils, have been isolated from the *T. ruticarpum* fruits.[1] Especially, among the main components of *T. ruticarpum* fruit, evodi-

Received: April 16, 2022
Accepted: June 14, 2022
Published: June 28, 2022

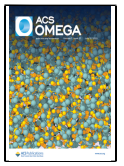

https://doi.org/10.1021/acsomega.2c02380
ACS Omega 2022, 7, 23736−23743

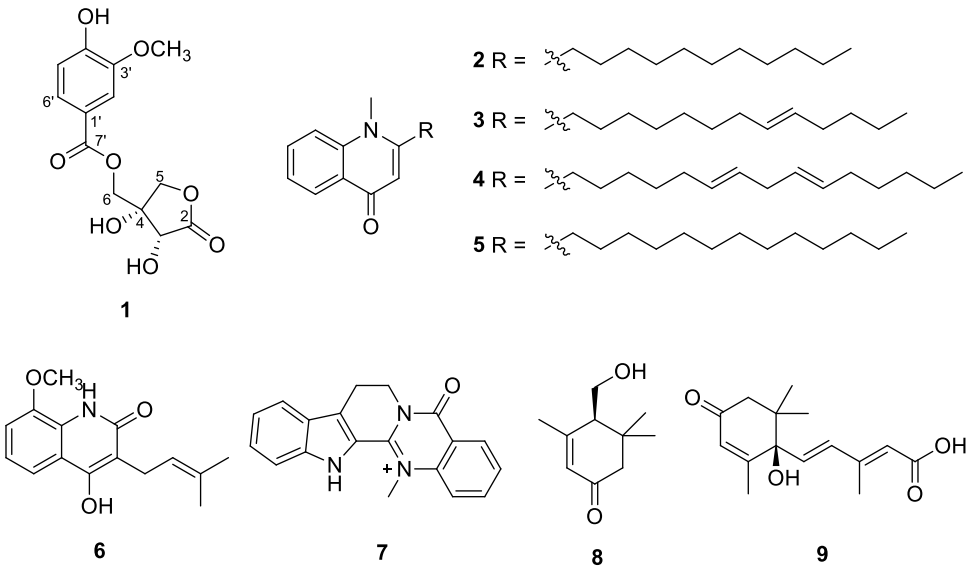

Figure 1. Chemical structures of compounds **1**−**9**.

amine and rutecarpine were found to act as partial agonists and antagonists of transient receptor potential vanilloid 1 (TRPV1).[10] In addition, rutecarpine has been reported to inhibit COX-2,[11] and evodiamine has been shown to possess anticancer activities both *in vitro* and *in vivo* by inhibiting proliferation, invasion, and metastasis by inducing apoptosis in various tumor cell lines.[12]

Of note, one of the major traditional uses of *T. ruticarpum* fruits is to treat gastric and duodenal ulcers, vomiting, and diarrhea,[1] and its traditional usage can be potentially associated with the antibacterial activity of *T. ruticarpum* fruits against *H. pylori*. To date, the antibacterial activity of *T. ruticarpum* fruit has been widely investigated. Quinolone alkaloids from *T. ruticarpum* fruits have been reported to inhibit the growth of *Mycobacterium fortuitum*, *Mycobacterium smegmatis*, and *Mycobacterium phlei*, indicating their therapeutic potential for tuberculosis.[13] Other quinolone alkaloids, euocarpines A-E, exhibit antibacterial activity against *Staphylococcus aureus* ATCC25923, *Staphylococcus epidermidis* ATCC12228, and *Bacillus subtilis* ATCC6633.[5] In addition, rhetsinine, an indole alkaloid, exhibits potent antibacterial activity against *Xanthomonas oryzae* pv. *oryzae*, *Xanthomonas oryzae* pv. *oryzicola*, and *Xanthomonas oryzae* pv. *oryzae*,[14] and essential oils derived from *T. ruticarpum* fruits exhibited antibacterial activity against *Bacillus subtilis* ATCC 6633 and *Staphylococcus aureus* ATCC 6538.[15] However, to the best of our knowledge, the antibacterial activity of *T. ruticarpum* fruits and their responsible components against *H. pylori* has not been investigated, although *T. ruticarpum* fruits have been used traditionally to treat gastric and duodenal ulcers. Thus, the anti-*H. pylori* compounds from *T. ruticarpum* fruits should be elucidated to support the therapeutic application of *T. ruticarpum* fruits in the treatment of gastric and duodenal ulcers.

As part of our continuing natural product discovery research for the identification of bioactive components from diverse natural resources,[16−20] we explored antibacterial components from an ethanolic (EtOH) extract of *T. ruticarpum* fruit. We performed solvent partition of EtOH extracts of *T. ruticarpum* fruit and applied the solvent-partitioned fractions to antibacterial activity tests in our bioactivity screening, where we observed that the CH_2Cl_2 fraction showed strong antibacterial activity against *Helicobacter pylori* strain 51. Intensive phytochemical investigation of the active CH_2Cl_2 fraction, aided by liquid chromatography−mass spectrometry (LC/MS)-based analysis, led to the isolation of nine compounds (**1**−**9**), including phellolactone (**1**), whose absolute configuration has not yet been determined. In this study, the chemical structure of phellolactone (**1**) was elucidated by conventional spectroscopic data analysis, including one-dimensional (1D) and two-dimensional (2D) nuclear magnetic resonance (NMR) and high-resolution electrospray ionization mass spectrometry (HR-ESIMS), as well as computational methods including electronic circular dichroism (ECD) calculations and the NOE/ROE-based interproton distance measurement technique via peak amplitude normalization for improved cross-relaxation (PANIC). Herein, we describe the separation and structural elucidation of compounds **1**−**9** and evaluation of their anti-*H. pylori* activity.

2. RESULTS AND DISCUSSION

2.1. Separation of Compounds from *T. ruticarpum* Fruit. Dried *T. ruticarpum* fruits were extracted with 50% EtOH under reflux, yielding a crude ethanolic extract by evaporation *in vacuo*. The resultant EtOH extract was sequentially subjected to solvent partitioning using four organic solvents: *n*-hexane, CH_2Cl_2, EtOAc, and BuOH. Four main solvent-partitioning fractions with increasing polarity were obtained: *n*-hexane-, CH_2Cl_2-, EtOAc-, and BuOH-soluble fractions. The LC/MS analysis of each fraction using reference to the in-house UV library database in our LC/MS system revealed that the CH_2Cl_2-soluble fraction mainly contains alkaloids and/or phenolic acids. In addition, the major traditional usage of *T. ruticarpum* fruits to treat gastric and duodenal ulcers can be potentially associated with the antibacterial activity of *T. ruticarpum* fruits against *H. pylori*, and thus the anti-*H. pylori* activities of *T. ruticarpum* fruit extract and its solvent-partitioning fractions were evaluated using a clinical strain of *H. pylori* 51 in our bioactivity screening test. Although the crude extract showed no inhibitory activity against *H. pylori* strain 51, the CH_2Cl_2-soluble fraction showed potent antibacterial activity against *H.*

https://doi.org/10.1021/acsomega.2c02380
ACS Omega 2022, 7, 23736−23743

pylori strain 51 with 94.3% inhibition at a final concentration of 100 μg/mL, which was comparable to that of the positive control, metronidazole (97.0% inhibition at a final concentration of 100 μM). Based on these results, the CH_2Cl_2-soluble fraction was subjected to phytochemical investigation by repeated column chromatography and semipreparative high-performance liquid chromatography (HPLC) with the guidance of LC/MS analysis, which led to the isolation of nine compounds (**1**–**9**) (Figure 1).

2.2. Structural Elucidation of the Isolated Compounds 1–9. Compound **1** was isolated as a white, amorphous powder. The molecular formula of **1** was established as $C_{13}H_{14}O_8$, determined by negative-ion HR-ESIMS, which revealed an $[M - H]^-$ ion peak at m/z 297.0618 (calcd. for $C_{13}H_{13}O_8$, 297.0610). The ^{1}H NMR data (Table 1) of compound **1**, assigned by the aid of heteronuclear single quantum correlation (HSQC) experiment, showed the presence of signals for one set of ABX signals at δ_H 7.61 (1H, dd, J = 8.0, 2.0 Hz, H-6′), 7.59 (1H, d, J = 2.0 Hz, H-2′), 6.86 (1H, d, J = 8.0 Hz, H-5′), indicating a 1,3,4-trisubstituted aromatic ring, two oxymethylene groups [δ_H 4.41 (1H, d, J = 10.0, H-5α)/4.26 (1H, d, J = 10.0, H-5β) and 4.39 (1H, d, J = 11.5, H-6a)/4.43 (1H, d, J = 11.5, H-6b)], an oxymethine group [δ_H 4.55 (1H, s, H-3)], and one methoxy group [δ_H 3.91 (3H, s, 3′-OCH_3)]. The ^{13}C NMR data (Table 1) of **1**, combined with heteronuclear multiple bond correlation (HMBC) experiment, revealed 13 carbon resonances, including six carbons for the aromatic ring; two carbonyl carbons at δ_C 166.2 and 176.2; four oxygenated carbons at δ_C 64.6, 70.1, 72.3, and 75.5; and one methoxy carbon at δ_C 54.9.

Table 1. ^{1}H (850 MHz) and ^{13}C NMR (212.5 MHz) Data for Compound 1 in CD_3OD (δ ppm)[a]

position	δ_H (J in Hz)	δ_C[b]
2		176.2 C
3	4.55 s	70.1 CH
4		75.5 C
5α	4.41 d (10.0)	72.3 CH_2
5β	4.26 d (10.0)	
6a	4.39 d (11.5)	64.6 CH_2
6b	4.43 d (11.5)	
1′		120.4 C
2′	7.59 d (2.0)	112.3 CH
3′		147.4 C
4′		151.8 C
5′	6.86 d (8.0)	114.6 CH
6′	7.61 dd (8.0, 2.0)	123.9 CH
7′		166.2 C
3′-OCH_3	3.91 s	54.9 CH_3

[a]Coupling constants (Hz) are given in parentheses. [b]^{13}C NMR data were assigned based on HSQC and HMBC experiments.

The planar structure of **1** was elucidated by interpretation of 2D NMR data (^{1}H–^{1}H COSY and HMBC). The ^{1}H–^{1}H COSY correlations of H-5′/H-6′ and HMBC correlations of H-2′/C-4′ and C-6′, H-5′/C-3′ and C-6′, and H-6′/C-1′ and C-3′, as well as the HMBC correlation of OCH_3/C-3′, confirmed the presence of a 1,3,4-trisubstituted aromatic ring. Importantly, the γ-lactone moiety was deduced from the key HMBC correlations of H-3/C-2 (δ_C 176.2), C-4 (δ_C 75.5), C-5 (δ_C 72.3), and C-6 (δ_C 64.6), and H-5/C-2, C-3 (δ_C 70.1), and C-6 (Figure 2). Furthermore, the γ-lactone moiety was connected to the aromatic ring via the linkage between C-6 and the ester moiety (C-7′), which was confirmed by the key HMBC correlations of H-6/C-7′, H-2′/C-7′, and H-6′/C-7′ (Figure 2). Based on the 2D NMR data, the complete planar structure of **1** was determined to be 2β,3β-dihydroxy-3α-vanilloylmethyl-γ-lactone, which was previously reported as phellolactone from *Phellodendron chinense* bark.[21] However, to the best of our knowledge, the absolute configuration of phellolactone has not yet been determined. Thus, it would be worthwhile to determine its absolute configuration.

First, the relative configuration of the γ-lactone moiety was established based on the NOESY experiment, where the cross-peak of H-5β/H-3 confirmed the hydroxyl group of C-3 to be in the α configuration (Figure 2). However, despite intensive NOESY data analysis of **1**, the configuration of the hydroxyl group at C-4 was not confirmed by the experimental spectroscopic data because it was difficult to distinguish the NOESY cross-peak between H-5 and H-6, and it was predicted that the NOESY correlation of H-3/H-6 could be detected in both the 4α-OH and 4β-OH cases as the interproton distance between H-3 and H-6 in **1** was calculated within 5.00 Å. The inversion of the 4-OH configuration significantly affected the conformational change of the γ-lactone moiety. Therefore, to accomplish a configurational analysis of the γ-lactone moiety, we applied the NOE/ROE-based interproton distance measurement technique via the PANIC method.[22−24] The PANIC-based calibrated interproton distance between H-3 and H-6b is 2.21 Å (Figure S10). To predict the interproton distance between H-3 and H-6b in the situation of 4α-OH or 4β-OH in **1**, molecular mechanics and quantum mechanics-optimized three-dimensional (3D) structures of **1A** (3α-OH and 4α-OH) and **1B** (3α-OH and 4β-OH) were generated and calculated. The predicted interproton distance between H-3 and H-6b of **1A** (2.34 Å) was matched well with the experimental value (2.21 Å), rather than **1B** (3.85 Å), which

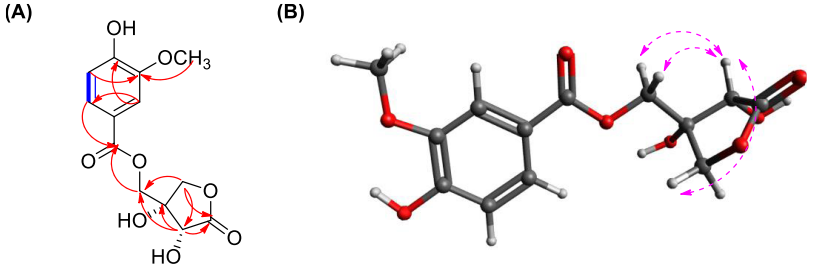

Figure 2. (A) Key ^{1}H–^{1}H COSY (blue hyphen) and HMBC (red forward-curved arrow) correlations for **1**. (B) Key nuclear Overhauser effect spectroscopy (NOESY) correlations of **1**.

https://doi.org/10.1021/acsomega.2c02380
ACS Omega 2022, 7, 23736−23743

suggested *cis*-configuration between 3-OH and 4-OH in **1** (Figure 3).

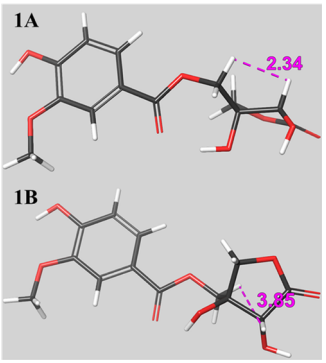

Figure 3. Optimized 3D structures of **1A** and **1B** with predicted interproton distance between H-3 and H-6b.

Finally, with reasonable structural elucidation of **1A**, the absolute configuration determination of **1** was confirmed by quantum chemical calculations for ECD simulations. Two possibilities with absolute configurations of 3*R*,4*R* and 3*S*,4*S* were calculated, and the experimental ECD spectrum of **1** was compared (Figure 4). The experimental ECD data were in good agreement with the calculated ECD data for (3*R*,4*R*)-**1**. Thus, the absolute configuration of the phellolactone isolated in this study was determined to be 3*R*,4*R* and compound **1** was named (3*R*,4*R*)-phellolactone.

The other isolated compounds were identified as 1-methyl-2-undecyl-4(1*H*)-quinolone (**2**),[25] 1-methyl-2-(8*E*)-8-tridecenyl-4(1*H*)-quinolinone (**3**),[26] 1-methyl-2-(6*Z*,9*Z*)-6,9-pentadecadien-1-yl-4(1*H*)-quinolinone (**4**),[26] dihydroevocarpine (**5**),[27] 4-hydroxy-8-methoxy-3-(3-methyl-2-buten-1-yl)-2(1*H*)-quinolinone (**6**),[28] dehydroevodiamine (**7**),[29] crocusatin C (**8**),[30] and (+)-*trans*-abscisic acid (**9**)[31] (Figure 1) by comparison of their NMR spectral and physical data with those reported earlier and the data from LC/MS analysis.

2.3. Evaluation of Antibacterial Activity of the Isolated Compounds against *H. pylori*. *H. pylori* is a major public health issue worldwide, affecting approximately 50% of the global population.[32] Eradication of *H. pylori* helps treat both gastric and duodenal ulcers, and even gastric cancer, because the presence of *H. pylori* is known to be associated with gastric or duodenal pathologies.[33] The antibacterial activity of *T. ruticarpum* fruits against *H. pylori* can be involved with the major traditional usage of *T. ruticarpum* fruits to treat gastric and duodenal ulcers. In our bioactivity screening test of the *T. ruticarpum* fruit extract and its derived fractions, we found that the CH_2Cl_2-soluble fraction showed potent antibacterial activity against *H. pylori* strain 51 with 94.3% inhibition. Next, compounds **1**−**9** isolated from the active CH_2Cl_2-soluble fraction were evaluated for antibacterial activity against *H. pylori* strain 51 (Table 2). Among the isolates, compound **3** exhibited the most potent antibacterial activity against *H. pylori* strain 51, with 94.4% inhibition at a final concentration of 100 μM, comparable to that of metronidazole (97.0% inhibition) as a positive control, and it showed MIC_{50} and MIC_{90} values of 22 and 50 μM, respectively. Compound **5** displayed moderate antibacterial activity against *H. pylori* strain 51 with 58.6% inhibition, which was higher than that of quercetin (34.4% inhibition) as a positive control, with an MIC_{50} value of 99 μM. The other

Table 2. Anti-*H. pylori* Activity of Compounds 1−9 against *H. pylori* Strain 51 Treated with 100 μM of Each Compound

compound	inhibition (%)	MIC_{50} (μM)	MIC_{90} (μM)
1	8.1		
2	0.0		
3	94.4	22	50
4	14.8		
5	58.6	99	>100
6	15.7		
7	20.0		
8	7.1		
9	16.1		
quercetin[a]	34.4		
metronidazole[a]	97.0	17	46

[a]Positive controls.

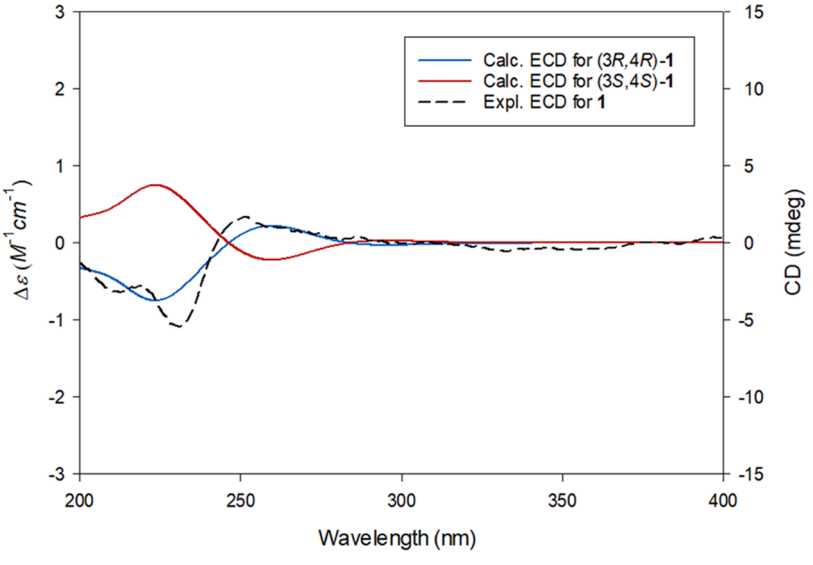

Figure 4. Experimental and calculated ECD spectra of compound **1**.

https://doi.org/10.1021/acsomega.2c02380
ACS Omega 2022, 7, 23736−23743

compounds showed weak activity or failed to exhibit anti-*H. pylori* infection, respectively (Table 2). Based on these findings, quinolone alkaloids (**3** and **5**) with 13 carbons on the side chain showed anti-*H. pylori* activity, and the presence of double bonds and the length of the side carbon chain in quinolone alkaloids may be important for anti-*H. pylori* activity. Interestingly, the structure−activity relationship analysis confirmed that this study corresponds exactly to previous studies showing that quinolone alkaloids with 13 carbons on the side chain are the most potent antibacterial compounds.[5] The mechanisms of anti-*H. pylori* activity include antiadhesion, oxidative stress to *H. pylori*, the inhibition of bacterial enzymes such as urease and *N*-acetyltansferase, and hydrophilic/hydrophobic interaction.[34,35] Further studies will be required to elucidate the exact mechanism by which active compounds **3** and **5** inhibit *H. pylori* growth. Effects of the active compounds on the human body with safety issues and their cytotoxicity to other cells are also required in the following study.

3. CONCLUSIONS

In this study, phytochemical investigation of the EtOH extract of *T. ruticarpum* fruits, a traditional herbal medicine used to treat gastric and duodenal ulcers, led to the isolation and identification of nine compounds (**1**−**9**), including phellolactone (**1**), whose absolute configuration has not yet been determined. The complete structure of phellolactone (**1**), including its absolute configuration, was elucidated using conventional spectroscopic data analysis, including 1D and 2D NMR and HR-ESIMS, and computational methods, including ECD calculation and NOE/ROE-based interproton distance measurement technique via the PANIC method. All of the compounds (**1**−**9**) were isolated from the anti-*H. pylori*-active CH_2Cl_2-soluble fraction, and from anti-*H. pylori* activity test of the isolates, compound **3** showed the most potent antibacterial activity against *H. pylori* strain 51, with 94.4% inhibition (MIC_{50} and MIC_{90} values of 22 and 50 μM, respectively), comparable to that of metronidazole (97.0% inhibition, and MIC_{50} and MIC_{90} values of 17 and 46 μM, respectively). Moreover, compound **5** exhibited moderate antibacterial activity against *H. pylori* strain 51, with 58.6% inhibition (MIC_{50} value of 99 μM), which was higher than that of quercetin (34.4% inhibition) as a positive control. Accordingly, the present study at least partially elucidated the antibacterial constituents from the *T. ruticarpum* fruits and revealed the anti-*H. pylori* principles, which provide the scientific basis of this plant as the herb in the folk application to treat gastric and duodenal ulcers.

4. EXPERIMENTAL SECTION

4.1. General Experimental Procedures. Optical rotations were measured using a JASCO P-2000 polarimeter (JASCO, Easton, MD). Ultraviolet (UV) spectra were acquired using an Agilent 8453 UV−visible spectrophotometer (Agilent Technologies, Santa Clara, CA). ECD spectra were obtained using a JASCO J-1500 spectropolarimeter (JASCO). Infrared (IR) spectra were recorded on a Bruker IFS-66/S FT-IR spectrometer (Bruker, Karlsruhe, Germany). NMR spectra were recorded with a Bruker AVANCE III HD 850 NMR spectrometer with a 5 mm TCI CryoProbe operating at 850 MHz (^{1}H) and 212.5 MHz (^{13}C), with chemical shifts given in ppm (δ) for ^{1}H and ^{13}C NMR analyses. All HR-ESIMS data were obtained using an Agilent G6545B quadrupole time-of-flight mass spectrometer (Agilent Technologies) coupled to an Agilent 1290 Infinity II high-performance liquid chromatography (HPLC) instrument using an Agilent Eclipse Plus C18 column (2.1 × 50 mm, 1.8 μm; flow rate: 0.3 mL/min). Preparative HPLC was performed using a Waters 1525 Binary HPLC pump with a Waters 996 Photodiode Array Detector (Waters Corporation, Milford, MA) and an Agilent Eclipse C18 column (250 × 21.2 mm, 5 μm; flow rate: 5 mL/min; Agilent Technologies). Semipreparative HPLC was performed using a Shimadzu Prominence HPLC System with SPD-20A/20AV Series Prominence HPLC UV−vis detectors (Shimadzu, Tokyo, Japan) and a Phenomenex Luna C18 column (250 × 10 mm, 5 μm; flow rate, 2 mL/min; Phenomenex, Torrance, CA). LC/MS analysis was performed on an Agilent 1200 Series HPLC system equipped with a diode array detector and 6130 Series ESI mass spectrometer using an analytical Kinetex C18 100 Å column (100 × 2.1 mm, 5 μm; flow rate: 0.3 mL/min; Phenomenex). Silica gel 60 (230−400 mesh; Merck, Darmstadt, Germany) and RP-C18 silica gel (Merck, 230−400 mesh) were used for column chromatography. Sephadex-LH20 (Pharmacia, Uppsala, Sweden) was used as the packing material for the molecular sieve column chromatography. Thin-layer chromatography (TLC) was performed using precoated silica gel F254 plates and RP-C18 F254s plates (Merck), and spots were detected under UV light or by heating after spraying with anisaldehyde-sulfuric acid.

4.2. Plant Material. Dried *T. ruticarpum* fruit was purchased from the Kyungdong herbal market in Seoul, Korea in July 2020, and the plant material was identified by one of the authors (K. H. Kim). A voucher specimen (OSU-2020) was deposited in the herbarium of the School of Pharmacy, Sungkyunkwan University, Suwon, Korea.

4.3. Extraction and Isolation. Completely dried fruits of *T. ruticarpum* (600 g) were extracted three times with 50% EtOH under reflux (2.0 L × 3) and then filtered. The filtrate was subsequently evaporated *in vacuo* to obtain the crude EtOH extract (172.7 g). The extract was dissolved in distilled water (1.0 L) and partitioned with hexane, dichloromethane (CH_2Cl_2), ethyl acetate (EtOAc), and *n*-butanol (*n*-BuOH). Four layers with increasing polarity, including hexane-, CH_2Cl_2-, EtOAc-, and *n*-BuOH-soluble fractions, were obtained as 1.2, 0.9, 2.1, and 18.7 g, respectively. Through TLC and LC/MS analysis of each fraction, we found that the CH_2Cl_2-soluble fraction (0.9 g) contains mainly alkaloids and/or phenolic acids, and in our bioactivity screening, the CH_2Cl_2-soluble fraction showed antibacterial activity against *H. pylori* strain 51. Thus, the CH_2Cl_2-soluble fraction was loaded onto a silica gel chromatography column and subjected to a gradient solvent system of CH_2Cl_2−MeOH (60:1−1:1, v/v) to give seven eluted fractions (M1−M7). Fraction M1 (487.7 mg) was subjected to medium-pressure liquid chromatography to obtain four fractions (M11−M14). The M11 fraction (100.5 mg) was subjected to Sephadex-LH20 column chromatography with 100% MeOH to obtain three fractions (M111−M113). Compounds **2** (0.9 mg, t_R = 28.4 min), **3** (0.5 mg, t_R = 31.9 min), **4** (0.7 mg, t_R = 34.1 min), and **5** (1.0 mg, t_R = 42.3 min) were isolated from subfraction M111 (11.6 mg) via semipreparative reversed-phase HPLC with 75% MeCN/H_2O (isocratic system, flow rate: 2 mL/min). The M12 fraction (168.6 mg) was subjected to C18 silica gel reversed-phase column chromatography to obtain five fractions (M121−M125). Compound **1** (0.4 mg, t_R = 36.5 min) was isolated

https://doi.org/10.1021/acsomega.2c02380
ACS Omega 2022, 7, 23736−23743

from subfraction M121 (12.9 mg) via semipreparative reversed-phase HPLC with 30% MeOH/H_2O (isocratic system, flow rate: 2 mL/min). Compound **8** (1.2 mg, t_R = 50.8 min) was isolated from subfraction M122 (57.1 mg) using semipreparative reversed-phase HPLC with 30% MeOH/H_2O (isocratic system, flow rate: 2 mL/min). Compounds **6** (0.8 mg, t_R = 99.8 min) and **9** (1.4 mg, t_R = 106.1 min) were isolated from subfraction M125 (44.4 mg) using semipreparative reversed-phase HPLC with 55% MeOH/H_2O (isocratic system, flow rate: 2 mL/min). Fraction M4 (229.7 mg) was subjected to C18 silica gel reversed-phase column chromatography to obtain six fractions (M41−46). The M45 fraction (134.7 mg) was subjected to Sephadex-LH20 column chromatography to obtain four fractions (M451−M454). Compound **7** (6.0 mg, t_R = 12.3 min) was isolated from subfraction M451 (62.1 mg) using semipreparative reversed-phase HPLC with 50% MeOH/H_2O (isocratic system, flow rate: 2 mL/min).

4.3.1. (3R,4R)-Phellolactone (1). White amorphous powder; $[\alpha]_D^{25}$ −85 (*c* 0.02 MeOH); UV (MeOH) λ_{max} (log ε) 203 (1.82), 222 (3.51), 264 (1.56), 269 (0.78); CD (MeOH) λ_{max} ($\Delta\varepsilon$) 212 (−0.07), 231 (−0.12), 251 (+0.04) nm; IR (KBr) ν_{max}: 3410, 1706, 1599, 1516, 1462 cm^{-1}; ^1H (850 MHz) and ^{13}C (212.5 MHz) NMR data (Table 1); HR-ESIMS (negative-ion mode) *m*/*z* 297.0618 $[M - H]^-$ (calcd for $C_{13}H_{13}O_8$, 297.0610).

4.4. PANIC Analysis. PANIC analysis was carried out according to a previously reported method, with slight modifications.[22] Slices of the 2D NOESY spectrum of **1** were obtained using the MestReNova software (version 14.1.2-25024). As a reference,[22] the interproton distance between two ortho-relationship aromatic protons, H-5′ and H-6′ ($r_{reference}$), was set as 2.5 Å. The corresponding NOE intensity ($NOE_{reference}$) was obtained by integrating the signal of H-5′ from the slice of 2D NOESY spectrum irradiated at H-6′ normalized to -1000. The NOE intensity of H-6b was acquired by irradiation at H-3 normalized to -1000 and integrated ($NOE_{unknown}$). The calibrated interproton distance ($r_{unknown}$) was calculated with the following equation

$$\frac{NOE_{unknown}}{NOE_{reference}} = \left(\frac{r_{reference}}{r_{unknown}}\right)^6$$

The MacroModel (version 2021-4, Schrödinger LLC) program was used to generate molecular mechanics (MM)- and quantum mechanics (QM)-optimized 3D structures and measure the specific interproton distance.[36]

4.5. ECD Calculation. Initial conformational searches were performed at the MMFF94 force field using the MacroModel (version 2021-4, Schrödinger LLC) program with a mixed torsional/low-mode sampling method, in which a gas phase with a 50 kJ/mol energy window and 10,000 maximum iterations were employed. The Polak−Ribiere conjugate gradient protocol was established with 10,000 maximum iterations and a 0.001 kJ $(mol\ Å)^{-1}$ convergence threshold on the root-mean-square gradient to minimize conformers. The conformers proposed in this study (found within 20 kJ/mol in the MMFF force field) were selected for geometry optimization using TmoleX 4.3.2 with the density functional theory settings of B3-LYP/6-31+G(d,p).[37]

ECD calculations for the (3*R*,4*R*)-**1** and (3*S*,4*S*)-**1** conformers (20 conformers each) were performed at an identical theory level and basis sets. The calculated ECD spectra were simulated by superimposing each transition, where σ is the bandwidth at a height of 1/e. ΔE_i and R_i are the excitation energy and rotatory strength for transition *i*, respectively.[37] In this study, the value of σ was 0.2 eV. The excitation energies and rotational strengths of the ECD spectra were calculated based on the Boltzmann populations of conformers, and ECD visualization was performed using SigmaPlot 14.0.

$$\Delta\epsilon(E) = \frac{1}{2.297 \times 10^{-39}} \frac{1}{\sqrt{2\pi\sigma}} \sum_A^i \Delta E_i R_i e^{[-(E-\Delta E_i)^2/(2\sigma)^2]}$$

4.6. *Helicobacter pylori* Culture. The clinical strain of *H. pylori* 51 was provided by the *H. pylori* Korean Type Culture Collection, School of Medicine, Gyeongsang National University, Korea. The strain was grown and maintained on Brucella agar (BD Co., Sparks, MD) supplemented with 10% horse serum (Gibco, New York). The culture conditions were 37 °C, 100% humidity, and 10% CO_2 for 2−3 days.

4.7. Determination of Minimal Inhibitory Concentration (MIC) Values. MICs were determined using the broth dilution method as previously reported.[38,39] Bacterial colony suspension (20 μL) equivalent to 2−3 × 10^8 CFU/ mL and 20 μL of twofold diluted test samples and controls were added to each well of a six-well plate containing Brucella broth medium supplemented with 10% horse serum. The final volume was 2 mL. After 24 h of incubation, the bacterial growth was evaluated by measuring the optical density at 600 nm using a spectrophotometer. The MIC_{50} and MIC_{90} values were defined as the lowest concentrations of samples at which bacterial growth was inhibited by 50 and 90%, respectively, and were calculated using Excel (Microsoft, Redmond, WA). All values were obtained from two independent experiments.

■ ASSOCIATED CONTENT

Supporting Information

The Supporting Information is available free of charge at https://pubs.acs.org/doi/10.1021/acsomega.2c02380.

HR-ESIMS, 1D and 2D NMR spectra of compounds **1**, and slice of 2D NOESY spectrum for PANIC (PDF)

■ AUTHOR INFORMATION

Corresponding Author

Ki Hyun Kim − *School of Pharmacy, Sungkyunkwan University, Suwon 16419, Republic of Korea;* orcid.org/0000-0002-5285-9138; Phone: +82-31-290-7700; Email: khkim83@skku.edu; Fax: +82-31-290-7730

Authors

Myung Woo Na − *School of Pharmacy, Sungkyunkwan University, Suwon 16419, Republic of Korea*

Se Yun Jeong − *School of Pharmacy, Sungkyunkwan University, Suwon 16419, Republic of Korea*

Yoon-Joo Ko − *Laboratory of Nuclear Magnetic Resonance, National Center for Inter-University Research Facilities (NCIRF), Seoul National University, Seoul 08826, Republic of Korea*

Dong-Min Kang − *College of Pharmacy and Research Institute of Pharmaceutical Sciences, Gyeongsang National University, Jinju 52828, Republic of Korea*

Changhyun Pang − *School of Chemical Engineering, Sungkyunkwan University, Suwon 16419, Republic of Korea;* orcid.org/0000-0001-8339-7880

https://doi.org/10.1021/acsomega.2c02380
ACS Omega 2022, 7, 23736−23743

Mi-Jeong Ahn − *College of Pharmacy and Research Institute of Pharmaceutical Sciences, Gyeongsang National University, Jinju 52828, Republic of Korea*

Complete contact information is available at: https://pubs.acs.org/10.1021/acsomega.2c02380

Author Contributions

⊥M.W.N. and S.Y.J. contributed equally to this work.

Notes

The authors declare no competing financial interest.

■ ACKNOWLEDGMENTS

This work was supported by National Research Foundation of Korea (NRF) grants funded by the Korean government (MSIT) (grant nos. 2019R1A5A2027340 and 2021R1A2C2007937).

■ REFERENCES

(1) Li, M.; Wang, C. Traditional uses, phytochemistry, pharmacology, pharmacokinetics and toxicology of the fruit of *Tetradium ruticarpum*: A review. *J. Ethnopharmacol.* **2020**, *263*, No. 113231.

(2) Shan, Q. Y.; Sang, X. N.; Hui, H.; Shou, Q. Y.; Fu, H. Y.; Hao, M.; Liu, K. H.; Zhang, Q. Y.; Cao, G.; Qin, L. P. Processing and polyherbal formulation of *Tetradium ruticarpum* (A. Juss.) hartley: phytochemistry, pharmacokinetics, and toxicity. *Front. Pharmacol.* **2020**, *11*, No. 133.

(3) Hu, X.; Li, D.; Chu, C.; Li, X.; Wang, X.; Jia, Y.; Hua, H.; Xu, F. Antiproliferative effects of alkaloid evodiamine and its derivatives. *Int. J. Mol. Sci.* **2018**, *19*, No. 3403.

(4) Ko, H. C.; Wang, Y. H.; Liou, K. T.; Chen, C. M.; Chen, C. H.; Wang, W. Y.; Chang, S.; Hou, Y. C.; Chen, K. T.; Chen, C. F.; Shen, Y. C. Anti-inflammatory effects and mechanisms of the ethanol extract of *Evodia rutaecarpa* and its bioactive components on neutrophils and microglial cells. *Eur. J. Pharmacol.* **2007**, *555*, 211−217.

(5) Wang, X. X.; Zan, K.; Shi, S. P.; Zeng, K. W.; Jiang, Y.; Guan, Y.; Xiao, C. L.; Gao, H. Y.; Wu, L. J.; Tu, P. F. Quinolone alkaloids with antibacterial and cytotoxic activities from the fruits of *Evodia rutaecarpa*. *Fitoterapia* **2013**, *89*, 1−7.

(6) Wang, T.; Wang, Y.; Kontani, Y.; Kobayashi, Y.; Sato, Y.; Mori, N.; Yamashita, H. Evodiamine improves diet-induced obesity in a uncoupling protein-1-independent manner: involvement of antiadipogenic mechanism and extracellularly regulated kinase/mitogen-activated protein kinase signaling. *Endocrinology* **2008**, *149*, 358−366.

(7) Cho, M. H.; Shim, S. M.; Lee, S. R.; Mar, W.; Kim, G. H. Effect of *Evodiae fructus* extracts on gene expressions related with alcohol metabolism and antioxidation in ethanol-loaded mice. *Food Chem. Toxicol.* **2005**, *43*, 1365−1371.

(8) Zhang, Y. N.; Yang, Y. F.; Yang, X. W. Blood-brain barrier permeability and neuroprotective effects of three main alkaloids from the fruits of *Euodia rutaecarpa* with MDCK-pHaMDR cell monolayer and PC12 cell line. *Biomed. Pharmacother.* **2018**, *98*, 82−87.

(9) Tian, K. M.; Li, J. J.; Xu, S. W. Rutaecarpine: a promising cardiovascular protective alkaloid from *Evodia rutaecarpa* (Wu Zhu Yu). *Pharmacol. Res.* **2019**, *141*, 541−550.

(10) Wang, S.; Yamamoto, S.; Kogure, Y.; Zhang, W.; Noguchi, K.; Dai, Y. Partial activation and inhibition of TRPV1 channels by evodiamine and rutaecarpine, two major components of the fruits of *Evodia rutaecarpa*. *J. Nat. Prod.* **2016**, *79*, 1225−1230.

(11) Moon, T. C.; Murakami, M.; Kudo, I.; Son, K. H.; Kim, H. P.; Kang, S. S.; Chang, H. W. A new class of COX-2 inhibitor, rutaecarpine from *Evodia rutaecarpa*. *Inflammation Res.* **1999**, *48*, 621−625.

(12) Jiang, J.; Hu, C. Evodiamine: a novel anti-cancer alkaloid from *Evodia rutaecarpa*. *Molecules.* **2009**, *14*, 1852−1859.

(13) Adams, M.; Wube, A. A.; Bucar, F.; Bauer, R.; Kunert, O.; Haslinger, E. Quinolone alkaloids from *Evodia rutaecarpa*: a potent new group of antimycobacterial compounds. *Int. J. Antimicrob. Agents* **2005**, *26*, 262−264.

(14) Su, X. L.; Xu, S.; Shan, Y.; Yin, M.; Chen, Y.; Feng, X.; Wang, Q. Z. Three new quinazolines from *Evodia rutaecarpa* and their biological activity. *Fitoterapia* **2018**, *127*, 186−192.

(15) Liu, S. S.; Liu, Z. X.; Wei, H.; Yin, Y. Y.; Zhang, Q. W.; Yan, L. H.; Wang, Z. M.; Yang, L. X. Chemical compositions, yield variations and antimicrobial activities of essential oils from three species of *Euodiae fructus* in China. *Ind. Crops Prod.* **2019**, *138*, No. 111481.

(16) Lee, S. R.; Kang, H.; Yoo, M. J.; Yu, J. S.; Lee, S.; Yi, S. A.; Kim, K. H. Anti-adipogenic pregnane steroid from a Hydractinia-associated fungus, *Cladosporium sphaerospermum* SW67. *Nat. Prod. Sci.* **2020**, *26*, 230−235.

(17) Yu, J. S.; Park, M.; Pang, C.; Rashan, L.; Jung, W. H.; Kim, K. H. Antifungal phenols from *Woodfordia uniflora* collected in Oman. *J. Nat. Prod.* **2020**, *83*, 2261−2268.

(18) Lee, S.; Ryoo, R.; Choi, J. H.; Kim, J. H.; Kim, S. H.; Kim, K. H. Trichothecene and tremulane sesquiterpenes from a hallucinogenic mushroom *Gymnopilus junonius* and their cytotoxicity. *Arch. Pharmacal Res.* **2020**, *43*, 214−223.

(19) Jo, M. S.; Lee, S.; Yu, J. S.; Baek, S. C.; Cho, Y. C.; Kim, K. H. Megastigmane derivatives from the cladodes of *Opuntia humifusa* and their nitric oxide inhibitory activities in macrophages. *J. Nat. Prod.* **2020**, *83*, 684−692.

(20) Lee, K. H.; Kim, J. K.; Yu, J. S.; Jeong, S. Y.; Choi, J. H.; Kim, J. C.; Ko, Y. J.; Kim, S. H.; Kim, K. H. Ginkwanghols A and B, osteogenic coumaric acid-aliphatic alcohol hybrids from the leaves of *Ginkgo biloba*. *Arch. Pharmacal Res.* **2021**, *44*, 514−524.

(21) Li, X. H.; Zhang, W. J.; Qi, H. Y.; Shi, Y. P. A new phenolic lactone from the bark of *Phellodendron chinense*. *Chin. Chem. Lett.* **2009**, *20*, 958−960.

(22) Oh, J.; Quan, K. T.; Lee, J. S.; Park, I.; Kim, C. S.; Ferreira, D.; Thuong, P. T.; Kim, Y. H.; Na, M. NMR-based investigation of hydrogen bonding in a dihydroanthracen-1(4H)one from *Rubia philippinensis* and its soluble epoxide hydrolase inhibitory potential. *J. Nat. Prod.* **2018**, *81*, 2429−2435.

(23) Lee, S.; Kim, C. S.; Yu, J. S.; Kang, H.; Yoo, M. J.; Youn, U. J.; Ryo, R.; Bae, H. Y.; Kim, K. H. Ergopyrone, a styrylpyrone-fused steroid with a hexacyclic 6/5/6/6/6/5 skeleton from a mushroom *Gymnopilus orientispectabilis*. *Org. Lett.* **2021**, *23*, 3315−3319.

(24) Oh, J.; Kim, N. Y.; Chen, H.; Palm, N. W.; Crawford, J. M. An Ugi-like biosynthetic pathway encodes bombesin receptor subtype-3 agonists. *J. Am. Chem. Soc.* **2019**, *141*, 16271−16278.

(25) Lee, S. W.; Chang, J. S.; Lim, J. H.; Kim, M. S.; Park, S. J.; Jeong, H. J.; Kim, M. S.; Lee, W. S.; Rho, M. C. Quinolone alkaloids from *Evodiae fructus* inhibit LFA-1/ICAM-1-mediated cell adhesion. *Bull. Korean Chem. Soc.* **2010**, *31*, 64−68.

(26) Sugimoto, T.; Miyase, T.; Kuroyanagi, M.; Ueno, A. Limonoids and quinolone alkaloids from *Evodia rutaecarpa* Bentham. *Chem. Pharm. Bull.* **1988**, *36*, 4453−4461.

(27) Kamikado, T.; Chang, C. F.; Murakoshi, S.; Sakurai, A.; Tamura, S. Isolation and structure elucidation of three quinolone alkaloids from *Evodia rutaecarpa*. *Agric. Biol. Chem.* **1976**, *40*, 605−609.

(28) Shobana, N.; Yeshoda, P.; Shanmugam, P. A convenient approach to the synthesis of prenyl-, furo-and pyrano-quinoline alkaloids of the rutaceae. *Tetrahedron* **1989**, *45*, 757−762.

(29) Lin, L. C.; Li, S. H.; Wu, Y. T.; Kuo, K. L.; Tsai, T. H. Pharmacokinetics and urine metabolite identification of dehydroevodiamine in the rat. *J. Agric. Food. Chem.* **2012**, *60*, 1595−1604.

(30) Li, C. Y.; Wu, T. S. Constituents of the pollen of *Crocus sativus* L. and their tyrosinase inhibitory activity. *Chem. Pharm. Bull.* **2002**, *50*, 1305−1309.

(31) Smith, T. R.; Clark, A. J.; Clarkson, G. J.; Taylor, P. C.; Marsh, A. Concise enantioselective synthesis of abscisic acid and a new analogue. *Org. Biomol. Chem.* **2006**, *4*, 4186−4192.

(32) McGee, D. J.; George, A. E.; Trainor, E. A.; Horton, K. E.; Hildebrandt, E.; Testerman, T. L. Cholesterol enhances *Helicobacter*

pylori resistance to antibiotics and Ll-37. *Antimicrob. Agents Chemother.* **2011**, *55*, 2897−2904.
(33) Chey, W. D.; Wong, B. C.; Gastroenterology P.P.C.o.t.A.C.o.. American college of gastroenterology guideline on the management of *Helicobacter pylori* Infection. *Am. J. Gastroenterol.* **2007**, *102*, 1808−1825.
(34) Wang, Y. C. Medicinal plant activity on *Helicobacter pylori* related diseases. *World J. Gastroenterol.* **2014**, *20*, 10368−10382.
(35) Kong, Y. H.; Zhang, L.; Yang, Z. Y.; Han, C.; Hu, L. H.; Jiang, H. L.; Shen, X. Natural product juglone targets three key enzymes from *Helicobacter pylori*: inhibition assay with crystal structure characterization. *Acta Pharmacol. Sin.* **2008**, *29*, 870−876.
(36) Lee, S.; Jeong, S. Y.; Nguyen, D. L.; So, J. E.; Kim, K. H.; Kim, J. H.; Han, S. J.; Suh, S. S.; Lee, J. H.; Youn, U. J. Stereocalpin B, a new cyclic depsipeptide from the antarctic lichen *Ramalina terebrata*. *Metabolites* **2022**, *12*, No. 141.
(37) Lee, S. R.; Seok, S.; Ryoo, R.; Choi, S. U.; Kim, K. H. Macrocyclic trichothecene mycotoxins from a deadly poisonous mushroom, *Podostroma cornu-damae*. *J. Nat. Prod.* **2019**, *82*, 122−128.
(38) Khalil, A. A. K.; Park, W. S.; Lee, J.; Kim, H. J.; Akter, K. M.; Goo, Y. M.; Bae, J. Y.; Chun, M. S.; Kim, J. H.; Ahn, M. J. A new anti-*Helicobacter pylori* juglone from *Reynoutria japonica*. *Arch. Pharmacal Res.* **2019**, *42*, 505−511.
(39) Amin, M.; Anwar, F.; Naz, F.; Mehmood, T.; Saari, N. Anti-*Helicobacter pylori* and urease inhibition activities of some traditional medicinal plants. *Molecules* **2013**, *18*, 2135−2149.

https://doi.org/10.1021/acsomega.2c02380
ACS Omega 2022, 7, 23736−23743